Microtubule Dynamics at the G_2/M Transition: Abrupt Breakdown of Cytoplasmic Microtubules at Nuclear Envelope Breakdown and Implications for Spindle Morphogenesis

Ye Zhai, Paul J. Kronebusch, Patrick M. Simon, and Gary G. Borisy

Laboratory of Molecular Biology, University of Wisconsin, Madison, Wisconsin 53706

Abstract. We recently developed a direct fluorescence ratio assay (Zhai, Y., and G.G. Borisy. 1994. *J. Cell Sci.* 107:881–890) to quantify microtubule (MT) polymer in order to determine if net MT depolymerization occurred upon anaphase onset as the spindle was disassembled. Our results showed no net decrease in polymer, indicating that the disassembly of kinetochore MTs was balanced by assembly of midbody and astral MTs. Thus, the mitosis-interphase transition occurs by a redistribution of tubulin among different classes of MTs at essentially constant polymer level.

We now examine the reverse process, the interphase-mitosis transition. Specifically, we quantitated both the level of MT polymer and the dynamics of MTs during the G_2/M transition using the fluorescence ratio assay and a fluorescence photoactivation approach, respectively. Prophase cells before nuclear envelope breakdown (NEB) had high levels of MT polymer (62%) similar to that previously reported for random interphase populations (68%). However, prophase cells just after NEB had significantly reduced levels (23%) which recovered as MT attachments to chromosomes were made (prometaphase, 47%; metaphase, 56%). The abrupt reorganization of MTs at NEB was corroborated by anti-tubulin immunofluorescence staining using a variety of fixation protocols. Sensitivity to nocodazole also increased at NEB. Photoactivation analyses of MT dynamics showed a similar abrupt change at NEB, basal rates of MT turnover (pre-NEB) increased post-NEB and then became slower later in mitosis.

Our results indicate that the interphase-mitosis (G_2/M) transition of the MT array does not occur by a simple redistribution of tubulin at constant polymer level as the mitosis-interphase (M/G_1) transition. Rather, an abrupt decrease in MT polymer level and increase in MT dynamics occurs tightly correlated with NEB. A subsequent increase in MT polymer level and decrease in MT dynamics occurs correlated with chromosome attachment. These results carry implications for understanding spindle morphogenesis. They indicate that changes in MT dynamics may cause the steady-state MT polymer level in mitotic cells to be lower than in interphase. We propose that tension exerted on the kMTs may lead to their lengthening and thereby lead to an increase in the MT polymer level as chromosomes attach to the spindle.

RADICAL transformations occur in the architecture of the cell as it undergoes the transitions from its growth period of interphase to its division period of mitosis and then back to interphase. The most obvious are the nuclear events of chromosome condensation and nuclear envelope breakdown (NEB)[1] and the cytoplasmic events of microtubule (MT) breakdown with the subsequent formation of the mitotic spindle. Upon the return to interphase, the overall processes are reversed with the decondensation of the chromosomes, nuclear envelope reformation, dissolution of the spindle, and reformation of the cytoplasmic MTs.

Although anti-tubulin immunofluorescence studies (DeBrabander et al., 1979; Aubin et al., 1980; Vandre et al.,

Please address all correspondence to G.G. Borisy, Laboratory of Molecular Biology, University of Wisconsin, Madison, WI 53706. Tel.: (608) 262-4570. Fax: (608) 262-1365.

The current address of Y. Zhai is the Department of Laboratory of Medicine, Box 0808, MCB230, University of California, San Francisco, CA 94103.

1. *Abbreviations used in this paper*: CCD, cooled charge-coupled device; kMT, kinetochore microtubule; MT, microtubule; NEB, nuclear envelope breakdown.

1984; Vandre and Borisy, 1986; Merdes et al., 1991; Waters et al., 1993) have provided a description of stages in the transformation of the cytoplasmic MT array at the interphase-mitosis transition, the mechanism of progression through the transition remains to be established. Cell cycle studies have indicated that the transformation of the MT array is likely to be controlled by activation of the cdc2 kinase (Belmont et al., 1990; Verde et al., 1990, 1992), possibly by modulating microtubule-associated binding proteins (Ookata et al., 1995) or severing proteins (Vale, 1991; McNally and Vale, 1993; Shiina et al., 1992, 1994). However, the relationship of these biochemical reactions to the overall transition process is unclear and basic questions have yet to be answered.

We recently developed a direct fluorescence ratio assay (Zhai and Borisy, 1994) to quantify MT polymer in individual cells so that cell cycle changes in polymer level could be measured. In that study we used the technique to determine if anaphase onset was accompanied by net MT depolymerization as a test of models of mitosis in which anaphase chromosome movement is driven by MT disassembly (Inoué and Sato, 1967; Margolis and Wilson, 1981; Koshland et al., 1988; Coue et al., 1991). Our results showed no net decrease in polymer, indicating that the mitosis-interphase (M/G_1) transition occurs by a redistribution of tubulin among different classes of MTs at essentially constant polymer level. We concluded that if anaphase chromosome movement is driven by MT disassembly, such depolymerization must be local rather than global.

Another approach to investigating the mechanism of transformation of the MT array is to determine if substantive changes occur in microtubule dynamics. Fluorescence photobleaching studies have shown that most microtubules turn over more rapidly in mitosis than in interphase (for review see Gelfand and Bershadsky, 1991). We have recently (Zhai et al., 1995) investigated the dynamics of MTs in the spindle using a photoactivation approach (Mitchison, 1989) taking care to differentiate the kinetics of the dynamics of the nonkinetochore MTs from the kinetochore MTs. We found that turnover of nonkinetochore MTs (non-kMTs) occurred with a $t_{1/2}$ of <1 min while the kinetochore MTs (kMTs) had a $t_{1/2}$ of ~ 5 min. These results suggested that MTs captured by a kinetochore are protected from the rapid turnover that the other MTs experience, consistent with the suggestion of selective stabilization first suggested by Kirschner and Mitchison (1986). Beyond stabilizing a subpopulation of existing MTs, some evidence exists that kinetochore interactions with MTs may actually promote MT polymerization. When chromosomes were extracted from metaphase cells by micromanipulation, the amount of MT polymer remaining in the cell decreased as based on MT length measurements from electron micrographs (Nicklas and Gordon, 1985). However, to study such phenomena routinely, a simpler assay for measuring MT polymer is needed.

We now use the fluorescence ratio assay to ask if the interphase-mitosis transition, like the mitosis-interphase transition, occurs by a redistribution of tubulin subunits among different MT classes at essentially constant polymer level. Are the MTs of the interphase network simply reorganized into the mitotic structure or are the interphase MTs first disassembled and then the spindle constructed from subunits? We also use fluorescence redistribution after photoactivation to measure MT turnover. We find that the level of MT polymer abruptly and transiently drops at NEB while the dynamics of MTs abruptly increase, findings that carry implications for spindle morphogenesis.

Materials and Methods

Cell Culture

Cells from the rat kangaroo epithelial line PtK_1 (American Type Culture Collection, Rockville, MD) were cultured in F-10 medium (Gibco Biological Company, Grand Island, New York) containing 10% FBS (Hyclone Laboratories, Logan, UT), 20 mM Hepes, and antibiotics. 2 d before an experiment, cells were transferred to an etched locator coverslip (Bellco Biotechnology, Bellco Glass, Inc. Vineland, NJ) mounted over a hole in the bottom of a 35-mm culture dish modified for microinjection (Gorbsky et al., 1987) and grown at 37°C in 5% CO_2. Cells from the porcine kidney epithelial cell line LLC-PK were cultured similarly but in Dulbecco's Modified Eagle's (DME) medium in 10% CO_2.

Preparation of Derivatized Tubulin and Microinjection

Xrhodamine derivatization of tubulin was performed as described previously (Sammak et al., 1987), and the preparation of caged-fluorescein tubulin was essentially as described by Mitchison (1989). The tubulin derivatives were distributed into 5-μl aliquots and stored in liquid nitrogen. Just before use, an aliquot was thawed and spun for 30 min at 20,000 *g*, 0°C to clarify the solution and prevent pipette clogging.

Microinjections were performed according to the protocols previously described (Zhai and Borisy, 1994). Xrhodamine tubulin used for microinjections to determine the proportion of MT polymer was in the concentration range 70–80 μM and a dye to protein molar ratio of 0.6:1.0. Caged fluorescein tubulin was prepared at a concentration of 150–200 μM and a dye to protein ratio of 0.3:1.0. To analyze MT turnover, we generally injected a mixture of xrhodamine tubulin (15 μM) and caged-fluorescein tubulin (120 μM) so that the entire MT population as well as the activated zone could be visualized. The volume injected was estimated at 5–10% of the cell volume. Prophase cells were injected and then incubated at 37°C for 15–25 min to allow copolymerization of injected and endogenous tubulin before imaging was begun. Interphase cells were allowed to incorporate label for 2 h at 37°C before imaging.

Cell Lysis and Tubulin Extraction

For determining the proportion of MT polymer, injected cells were imaged and then lysed and extracted in a MT-stabilizing buffer, PHEM, (60 mM Pipes, 25 mM Hepes, 10 mM EGTA, 2 mM $MgCl_2$, pH 6.9) containing 0.5% Triton X-100 (Pierce, Rockford, IL) detergent and 10 μg/ml taxol as described previously (Zhai and Borisy, 1994). Taxol was included to specifically stabilize MTs during extraction, and to maintain their stability during subsequent processing. After cell lysis and tubulin extraction, the cells were immediately returned to the microscope stage, relocated by means of the etched locator grid and imaged again.

Immunofluorescence

For immunostaining, cells were rinsed with PBS, pH 7.2 at 37°C and lysed and extracted for 1–2 min in 0.2% Triton X-100 in PHEM supplemented with 10 μg/ml taxol (National Cancer Institute, Bethesda, MD) in order to stabilize MTs. The cells were then fixed with a variety of fixation methods: (*a*) 2% glutaraldehyde, (*b*) 4% formaldehyde, or (*c*) 5 mM ethylene glycol *bis*-(succinic acid *N*-hydroxy succinimide ester) (EGS) (Pierce, Rockford, IL) all in PHEM at 37°C for 30 min. The coverslips then were removed from the dish after rinsing in PBS and cells were further permeabilized by soaking in 0.2% Triton X-100 in PBS for 1–5 min. For glutaraldehyde fixed cells, the free aldehyde groups were reduced by three soaks, 10 min each, in fresh solutions of 1 mg/ml $NaBH_4$ in PBS.

To prevent possible loss of labile MTs during lysis and extraction, we also used different procedures in which cells were first fixed, and then lysed and extracted. Cells were fixed with (*d*) methanol for 10 min at −20°C, or with (*e*) glutaraldehyde, (*f*) formaldehyde, or (*g*) EGS (Gorbsky et al., 1987) as described above. Then, the cells were rinsed with PBS and lysed

and extracted for 1–5 min in 0.5% Triton X-100 in PBS. For glutaraldehyde fixed cells, the free aldehyde groups were reduced by three soaks, 10 min each, in fresh solutions of 1 mg/ml $NaBH_4$ in PBS. In experiments where antibodies to lamin B were used, fixation was by rapid immersion in 100% cold (−20°C) methanol for 10 min. The fixation was followed by a 1-min lysis and extraction by 0.5% Triton X-100 in PHEM and a rinse in PBS. The coverslips were then processed for immunofluorescence.

Immunofluorescence was performed at 37°C by the following steps, each of which were separated by four 10-min rinses with PBS: (*1*) incubation with 10% goat serum in PBS for 30 min; (*2*) rat monoclonal (YL 1/2) anti-α-tubulin antibody (Accurate Chem. & Sci. Corp., Westbury, NY) or mouse monoclonal anti-β-tubulin antibody (Amersham Corp., Arlington Heights, IL) at 1:500 dilution in 1% goat serum/PBS, 60 min; (*3*) goat anti-mouse IgG:fluorescein, or goat anti-rat IgG:Texas red (Jackson Immuno Research, West Grove, PA) at 1:100 in 1% goat serum/PBS for 45 min. For lamin B staining experiments, the primary antibodies used were the rat monoclonal anti-α-tubulin and a mouse monoclonal anti-lamin B (Oncogene Science, Cambridge, MA).

Secondary antibodies were donkey anti-mouse IgG-conjugated with fluorescein and donkey anti-rat IgG-conjugated with Texas red (Jackson Immuno Research). The donkey antibodies were cross immunoadsorbed for rat and mouse serum, respectively. Finally, samples were mounted in Aqua-PolyMount (Polysciences Inc, Warrington, PA).

Data Collection and Image Analysis

Instrumentation and experimental procedures for collecting digital fluorescence images as well as quantitation of the proportion of MT polymer were as previously described (Zhai and Borisy, 1994). Photoactivation experiments were performed using the 334–364-nm bands of a 3 Watt argon ion laser (Spectra-Physics, Mountain View, CA) equipped with UV transmitting optics, and a Zeiss IM35 inverted microscope with a 100×, 1.3 NA Neofluor objective (Carl Zeiss, Inc., Thornwood, NY). The laser beam was directed into the epi-illumination port while the UV filter cassette was in the light path and aligned with respect to crosshairs in the optical path. Before photoactivation, the injected cell was located and positioned relative to the laser irradiation beam using phase contrast optics. We verified that the centrosomal MTs were fully labeled and of normal morphology by observation in the xrhodamine channel before activation. A pre-activation image in the fluorescein channel was routinely recorded. The cell was then activated by laser irradiation (20–40 mW) for 30–100 ms. Fluorescence images (0.2–1.0 s) and phase images were collected with a cooled charge-coupled device (CCD) (model CH220, Photometrics Ltd., Tucson, AZ) as soon as possible after photoactivation (5–10 s) and then at 20-s intervals. The medium in the culture dish was maintained at the experimental temperature (30°C for prophase cells 37°C for others) by circulating warm water through a brass block holding the dish chamber and through a coil surrounding the objective. A layer of mineral oil (E.R. Squibb and Sons Inc., Princeton, NJ) was overlaid on the medium to retard gas exchange and evaporation during observations.

Quantitation of the photoactivation data was performed using Photometrics CCD 200 software. The fluorescent images were first flat-fielded to make corrections for uneven illumination. Images were then displayed on the video monitor, a rectangle was delineated to surround the activated zone, and the fluorescence intensity values of the pixels within the rectangle were integrated. The intensity value obtained from a rectangle of the same size placed in a similar, but nonactivated region of the cell, was used as the background value and subtracted from the activated zone value. For interphase cells this region was a perinuclear region on the opposite side of the nucleus, for prophase cells it was the opposite centrosome, and for metaphase cells it was in the opposite half spindle. Intensity values at successive time points were normalized to the initial image value (time zero) and were fitted to a double exponential equation: $I = P_f\exp(-k_f t) + P_s\exp(-k_s t)$, where I = proportion of initial intensity of fluorescence; P_f = proportion of fluorescence decay due to fast process; k_f = rate constant for fluorescence decay (fast process); P_s = proportion of fluorescence decay due to slow process; k_s = rate constant for fluorescence decay (slow process). Double exponential regression analysis of the data was performed using SIGMAPLOT software (Jandel Scientific, Corte Madera, CA). Statistical analysis of MT polymer levels during the G_2/M transition were calculated with an analysis package (SAS Institute Inc., Cary, NC). For image processing and presentation, digital images were scaled to 8-bits using Image-1 video processing software (Universal Imaging Corp., Westchester, PA). Digital files were printed on a dye-sublimation, Digital Phaser II color printer (Tektronix, Inc., Wilsonville, OR).

Results

Four experimental approaches were taken to evaluate changes in MT assembly and dynamics at the G_2/M transition: (*a*) the proportion of MT polymer was determined using a fluorescence ratio assay method; (*b*) the lability of MTs was assessed by stabilization and sensitivity assays; (*c*) MT reorganization was studied by anti-tubulin immunofluorescence staining using a variety of fixation protocols; and (*d*) the dynamics of MT turnover was determined by analysis of dissipation of fluorescence after photoactivation.

Determination of the Proportion of MT Polymer

Initially, we investigated whether the G_2/M transition of MTs occurred by a redistribution of tubulin at constant polymer level as we previously reported for the mitosis-interphase transition (Zhai and Borisy, 1994). To examine the G_2/M transition, we used a fluorescence ratio assay which compares the fluorescence of xrhodamine tubulin in living cells to the fluorescence in the same cells after lysis and extraction to remove the soluble tubulin. PtK_1 cells in early prophase were microinjected with xrhodamine tubulin, and incubated at 37°C for at least 15–20 min to allow injected tubulin to incorporate into the MTs. Previous studies have demonstrated that the half-time of MT turnover in interphase cells is ~5 min (Saxton et al., 1984); thus, >15–20 min allows 3–4 half-times for label to equilibrate. Total tubulin fluorescence in individual, living cells was quantified using a cooled, scientific grade CCD image sensor. Cells were then washed and lysed into a MT-stabilizing buffer to extract the soluble pool. Total tubulin polymer fluorescence was determined for the extracted cells in the same way as for living cells. Quantitation of fluorescence in the living state gives a value proportional to total tubulin content: polymer plus the subunit pool. After extraction of the soluble subunit pool, the remaining fluorescence gives a value proportional to tubulin in polymer form. The ratio of fluorescence, extracted/living, then gives the proportion of tubulin in microtubules. Typical examples of the determination of MT polymer levels during the G_2/M transition are shown in Fig. 1. Total fluorescence intensity of tubulin in the cell was determined by integrating the intensity values for all the pixels within a rectangle surrounding the entire cell before and after lysis and extraction. The fluorescence image of the living cells showed fibrillar fluorescence over a diffuse background. Lysis and extraction decreased the diffuse background to a negligible level. We interpret the diffuse background as resulting from the soluble tubulin which is removed by the lysis and extraction procedure. We found that the average proportion of tubulin polymer dropped abruptly at NEB to 38% of its pre-NEB level and then gradually recovered as the cells progressed toward metaphase (Fig. 2 and Table I). Thus, in contrast to the mitosis-interphase transition which occurs at approximately constant polymer level, the interphase-mitosis transition showed a sharp transient. Since the focus of our study will be on the events surrounding this transition point of NEB, we will refer to late prophase cells as pre-NEB cells and to early prometaphase cells before spindle formation as post-NEB cells.

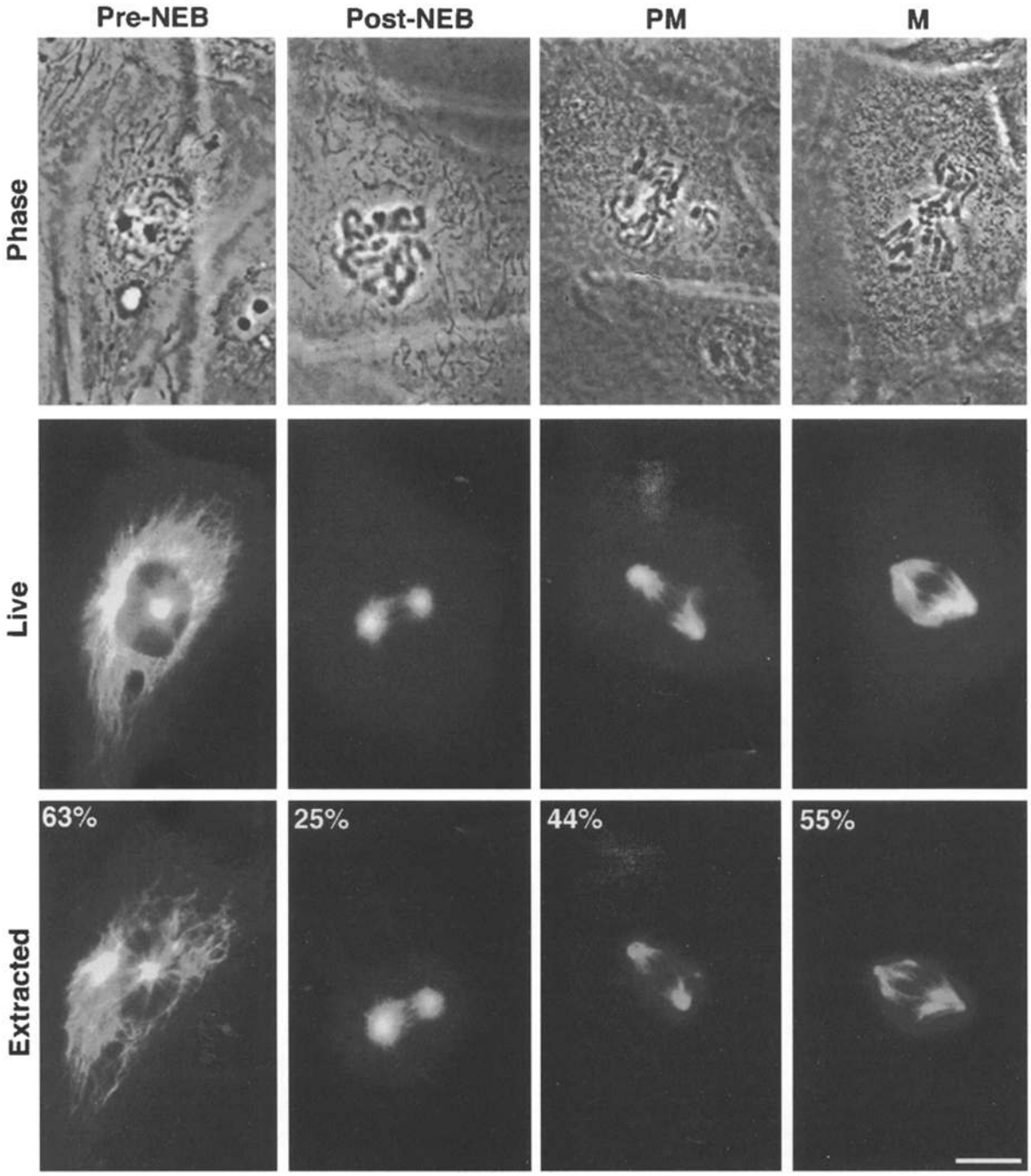

Figure 1. Ratiometric imaging of tubulin polymer at the G_2/M transition. Phase images of living cells (*top row*), total xrhodamine tubulin fluorescence of live cells (*middle row*), and xrhodamine MT polymer after cell lysis and extraction (*bottom row*) are shown for cells at four stages of the G_2/M transition at 37°C. Before nuclear envelope breakdown (*Pre-NEB*) long MTs radiate out from the centrosomes and extend to the edges of the cell. Immediately after nuclear envelope breakdown (*Post-NEB*) the cytoplasm of the living cells is filled with diffuse tubulin fluorescence and lysis reveals only short astral MTs radiating from the centrosomes. During later stages of prometaphase (*PM*) bundles of MTs extending from the poles to the chromosomes are seen in addition to the astral array of MTs. At metaphase (*M*) these kinetochore fibers are the most prominent MT structures seen in the cell. The level of MT polymer for each of the cells is shown in the upper left corner of images in the bottom row. Bar, 10 μm.

Evaluation of the Transient Drop in MT Polymer at NEB

A serious consideration is whether the fluorescence ratio results reflected a real decrease of MT polymer in the cells or merely an increased MT sensitivity to the lysis procedure at this stage. The dynamics of MTs are substantially greater in mitosis than in interphase (Saxton et al., 1984; Pepperkok et al., 1990; Zhai et al., 1995) and it seemed possible that a greater fraction of the mitotic MTs were lost, leading to an apparent but not real drop. Therefore,

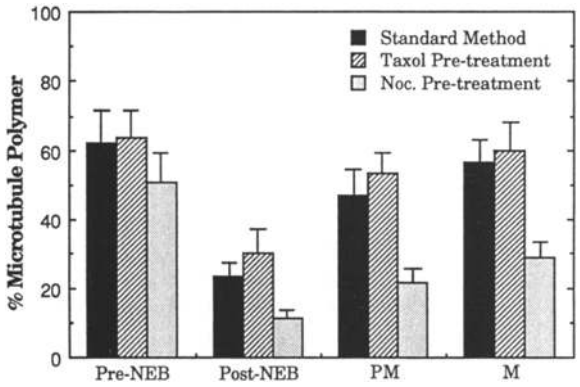

Figure 2. Quantitation of MT polymer at the G_2/M transition. Cells at the G_2/M transition have been grouped into four stages and the polymer level values are presented in histogram form. The four stages are : (*1*) prophase cells before nuclear envelope breakdown (*Pre-NEB*); (*2*) immediately after nuclear envelope breakdown and before spindle formation (*Post-NEB*); (*3*) prometaphase (*PM*), when a bipolar spindle has formed but not all chromosomes are properly aligned; and (*4*) metaphase (*M*) when all the chromosomes are aligned at the equator of the spindle. The standard lysis method revealed a dramatic decrease in polymer level as cells progressed from Pre-NEB to Post-NEB. Polymer levels were also determined in MT stabilization and sensitivity assays (see text) after brief treatment (45 s) with either taxol (10 μg/ml) or nocodazole (10 μg/ml).

to test this possibility, we carried out stabilization and sensitivity assays.

The rationale for the stabilization assay was to render all MTs stable before lysis so as to mitigate possible variation in loss of MTs during lysis. We stabilized pre-existing MTs by treating the cells with taxol (10 μg/ml) for 45 s before lysis and extraction and determined the polymer ratio as before (Fig. 2 and Table I). (Previous experiments had shown that taxol treatments longer than 45 s start to induce abnormal assembly [Zhai and Borisy, 1994].). After this brief drug treatment, polymer levels in taxol-treated pre-NEB cells were similar to those in untreated cells, 3% greater, which is within experimental error. Taxol-treated post-NEB cells showed a 29% higher level, which is statistically significant, indicating that some MTs were lost at this stage during the standard extraction procedure but, more importantly, the cells still exhibited a sharp drop in MT polymer at NEB, determined by this experimental design to be 47% of the pre-NEB value. Taxol-treated prometaphase and metaphase cells showed smaller variances from the untreated cells, 14% and 6%, respectively, indicating a recovery of MT stability as mitosis progressed.

The complementary approach was to assess MT sensitivity by blocking polymerization, thus inducing net depolymerization. This assay would evaluate possible changes in MT lability at NEB. For this assay, cells were treated with nocodazole (10 μg/ml) for 45 s before lysis and extraction, and then total tubulin polymer fluorescence was determined for the extracted cells as described above. Cells at different phases showed different decreases in their MT polymer level (Fig. 2 and Table I). Nocodazole-treated pre-NEB cells were only slightly affected, retaining 82% of the MT polymer of the untreated cells. This is

Table I. The Proportion of Microtubule Polymer at the G_2/M Transition

Experimental condition	Pre-NEB	Post-NED	PM	M
	%	%	%	%
Standard	61.9 ± 9	23.4 ± 3.8	47 ± 7.8	56.4 ± 6.9
Lysis method	(11)*	(10)	(5)	(10)
Taxol treatment	63.6 ± 8.7	30.3 ± 6.8	53.5 ± 6.5	59.7 ± 8.3
Before lysis	(13)	(11)	(11)	(14)
Noc. treatment	50.7 ± 8.4	11 ± 1.7	21.4 ± 4.7	28.7 ± 4.8
Before lysis	(8)	(9)	(12)	(11)

*Number of cells is shown in parentheses.
Cells at the G_2/M transition are grouped into four stages: pre-NEB, post-NEB, PM, and M as described in Fig. 2. The polymer level values obtained from different experimental protocols are listed.

similar to the behavior of interphase cells which lose MTs gradually in the presence of nocodazole. Overall the MT pattern observed in the extracted prophase cells after nocodazole treatment was similar to the pattern in the live cells before drug treatment with no preferential loss of centrosomal MTs. In contrast, nocodazole had a drastic effect on post-NEB cells where the polymer level dropped to 47% of the value of untreated cells. Usually only a small spot of fluorescence remained at the centrosomes. Some of the polymer that remained appeared to be one or two short bundles (perhaps newly formed kinetochore fibers that formed when astral MTs were captured and stabilized by chromosomes before the nocodazole treatment). Prometaphase and metaphase cells lost their astral MTs very quickly in nocodazole and the kinetochore MTs began to shorten as reported in other studies (Cassimeris et al., 1990; Centonze and Borisy, 1991). Polymer levels in these cells also fell to approximately half the value in untreated cells.

Two conclusions can be drawn from these stabilization and sensitivity experiments. The taxol stabilization experiments confirmed the abrupt and transient drop in MT polymer at NEB seen with the standard extraction protocol, although the magnitude of the drop was slightly less. Both the taxol stabilization and the nocodazole sensitivity experiments confirmed a substantial change in MT lability at NEB. Because of this apparent abrupt change in lability, a re-examination of the structural changes of the MT network accompanying the interphase-mitosis transition seemed warranted.

Immunofluorescence Evaluation of MT Reorganization at NEB

We used tubulin immunofluorescence to determine whether the xrhodamine images of injected cells were faithfully reporting the MT patterns in these cells, especially at the post-NEB stage. Although many publications (DeBrabander et al., 1979; Aubin et al., 1980; Vandre et al., 1984; Merdes et al., 1991) have described the MT network in interphase and mitotic cells, few report details of possible intermediates in the transition process. If the transition is abrupt, intermediates would be rare and could escape detection. We wondered if a detailed structural examination would confirm the apparent drop in MT polymer indicated by the fluorescence ratio assay. Consequently, we chose to re-examine the transition process. Because of the

lability of MTs immediately post-NEB, we were concerned that fixation conditions might not accurately preserve the labile MTs. Therefore, we explored a range of immunofluorescence protocols including fixation before as well as after lysis with detergent. Fixatives included glutaraldehyde, formaldehyde, EGS, and methanol as described in Materials and Methods.

The clearest images of the microtubule network came from cells that were lysed and extracted before fixation. Protocols involving fixation before cell lysis gave higher backgrounds of fluorescence in the cytoplasm, presumably because of retention of the soluble tubulin. Both classes of protocol, however, yielded the same overall sequence of events. Similar results were obtained with each of the fixatives used.

Interphase mammalian cells in culture are characterized by long microtubules that extend to the cell periphery. Many of these MTs may be tracked back towards the centrosome but many course through the cytoplasm without any obvious centrosomal connection. The transition of interphase cells to mitosis first becomes apparent in the MT network in early prophase. The early prophase stage appears to be primarily an interphase network which has been modified by an increased nucleation of MTs from the centrosome. Late prophase is an interphase-like network containing two separated centrosomes. A radial array of MTs develops focused on the centrosome that is more pronounced than in interphase and many of these MTs extend all the way to the margin of the cell. Prophase cells still contain many MTs which do not converge on either centrosome. Near the time of nuclear envelope breakdown at the transition from prophase to early prometaphase (just post-NEB), there is a radical change in the MT pattern. After this stage, the interphase-like MT array is no longer seen in the cytoplasm and centrosomal MTs which extended to the cell boundary in prophase now appear as short MTs about 5–10 μm in length. The rare cells fixed in this brief transition stage exhibit brightly staining asters with only a few long MTs or MT fragments scattered throughout the cytoplasm. Also, nonextracted fixed cells display a bright, cytoplasmic background, suggesting an increased soluble tubulin pool. Prometaphase cells contain short brightly staining asters in a cytoplasm that is otherwise devoid of MTs. Bundles of kinetochore MTs begin to appear at this stage as chromosomes capture astral MTs. The metaphase cell usually exhibits a high density of MTs within the spindle and an astral array that seems less pronounced. This description of MT re-arrangement as cells transit from interphase to mitosis is consistent with many previous studies (Rattner and Berns, 1976; DeBrabander et al., 1979; Aubin et al., 1980; Vandre et al., 1984; Vandre and Borisy, 1986; Merdes et al.,1991; Waters et al., 1993). Since we, as well as others, have observed these MT patterns using a variety of fixation methods (see Materials and Methods) both with pre-extraction (procedures: a, b, and c) and without pre-extraction (procedures: d, e, f, and g), it seems that the xrhodamine tubulin images shown in Fig. 1 faithfully represent the MT distributions that are seen in fixed cells. The decrease in the MT polymer level found at the post-NEB stage by the fluorescence ratio assay correlates with the sudden loss of cytoplasmic MTs and increase in background tubulin as seen by immunofluorescence. Thus, the immunofluorescence results are consistent with the conclusion that an abrupt drop in MT polymer occurs about the time of NEB.

The correlation between MT reorganization and NEB prompted the question of whether the timing of MT reorganization was determined by the process of NEB. To answer this question, the precise timing of these two events in the same cell needed to be evaluated, necessitating unambiguous assays for NEB in addition to MT reorganization. Since phase contrast optics often fail to reveal clearly the state of the nuclear envelope in fixed preparations, especially after they have been detergent extracted, we used the presence of the inner nuclear membrane protein, lamin B, as a molecular marker for the integrity of the nuclear envelope. Reorganization of the cytoplasmic MT network was defined primarily by loss of MTs from the cell periphery. Cells were fixed and labeled with primary antibodies to α-tubulin and lamin B (Fig. 3). Every prophase cell identified using phase contrast optics was imaged and examined for its MT and lamin B morphology. In all cases observed where the nucleus was intact as determined by lamin B fluorescence, (n = 123), the cytoplasmic MT network was intact as well (Fig. 3 *A*), indicating that breakdown of the cytoplasmic MTs does not precede NEB. In this survey, we found four cells in which the nucleus was determined to be in the process of breaking down as judged by intermediate levels of lamin B fluorescence and the appearance of rough edges in the lamin B pattern, indicative of a fragmentation event (Fig. 3 *B*). In all four examples identified, the MT network was still intact indicating that there was either some delay after onset of NEB before the reorganization of the MT network, or that both processes were initiated at the same time but NEB was rapid in comparison with MT reorganization. After NEB, the lamin B staining was either absent or in a vesiculated pattern (Fig. 3 *C*). From the duration of prophase (30 min) and the frequency with which nuclear envelope transition intermediates were observed in the prophase population (4/127 = .031), the duration of the NEB process may be estimated as ~1 min. The results indicate that the microtubule network begins reorganization at or shortly after the onset of NEB.

To determine the kinetics of microtubule reorganization post-NEB more precisely, correlated time-lapse microscopy and immunostaining was carried out. Cells in late prophase were located and closely monitored by phase contrast microscopy, recording images of all cells every 6 s in time-lapse mode to an optical memory disc recorder for subsequent playback analysis. Cells were then fixed at a stage that appeared by live observation to be the onset of NEB or they were allowed to progress 1 or 2 min beyond apparent NEB and were then fixed. After fixation, all cells were prepared for double immunofluorescence staining for tubulin and lamin B as described above (Table II). Of cells fixed at the apparent onset of NEB as judged by live cell observation, 40% had clearly undergone NEB as determined by reduced or fragmented lamin B staining but none had reorganized their microtubule network. Of cells fixed 1 min after the apparent onset of NEB, all had indeed completed NEB as assessed by lamin B staining, but only 40% of the cells were clearly in the process of cytoplasmic MT reorganization. At 2-min post-apparent NEB,

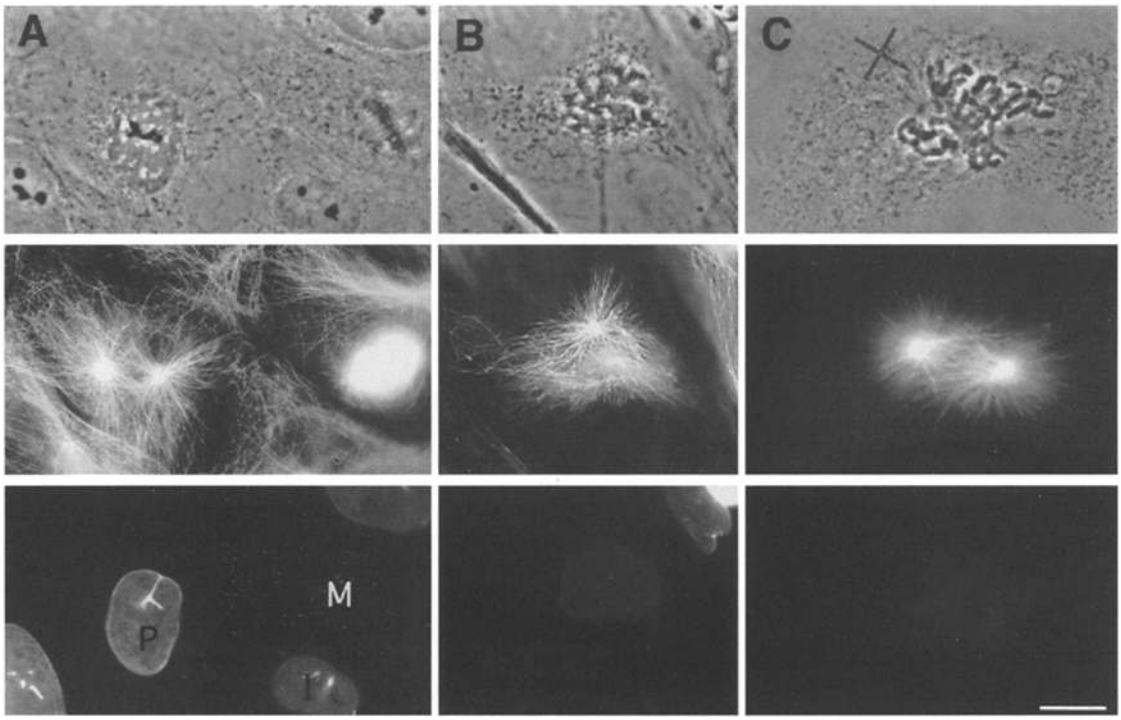

Figure 3. Microtubule and lamin B staining at prophase, NEB and post-NEB. For each stage the phase image (*top row*), anti-tubulin (*middle row*), and anti-lamin B (*bottom row*) staining patterns are shown. (*A*) Lamin B staining is as strong in a prophase cell (*P*) as it is in an interphase cell (*I*), while in a metaphase cell (*M*) the lamin B is dispersed throughout the cytoplasm and is not detectable in this print. Many long MTs radiate out from the prophase centrosomes and fill the cytoplasm as in interphase. (*B*) A cell in the process of NEB. Near the time of NEB the nuclear lamin B staining becomes weaker and NEB is indicated in this cell by the breaks in the staining of the nuclear envelope (upper part of the nucleus) and the absence of crisp nuclear edge staining (lower part of nucleus). At this stage, MTs still extend from the centrosomes to the cell periphery. Noncentrosomal MTs are also evident at the left edge of this cell. (*C*) A large cell fixed shortly after NEB. Weak lamin B staining appears in vesicles in the nuclear area and has not yet dispersed throughout the cytoplasm. Centrosomal MTs are relatively short and most of the cytoplasm is devoid of MTs. The position of the crosshairs in the phase image have no significance for this figure. All the lamin B figures were printed so interphase nuclei present in the original uncropped figures were at the same brightness. Bar, 10 μm.

again all cells had completed NEB as based on lamin B staining. At this time, all cells had also extensively reorganized their MT networks. These results establish that the process of NEB is indeed rapid, progressing to completion within 1 min and that breakdown of cytoplasmic MTs is also abrupt, occurring within ~2 min after the onset of NEB.

Photoactivation Analysis of MT Dynamics

Since the taxol stabilization and nocodazole sensitivity experiments indicated an abrupt increase in MT lability at NEB, we attempted to determine quantitatively the timing and degree of increase in MT dynamics. Previous studies (Saxton et al., 1984; Belmont et al., 1990; Pepperkok et al., 1990) have compared interphase and mitosis but have not examined NEB specifically. Dissipation of fluorescence after photoactivation was taken as the method of choice because of the inherently greater signal-to-noise ratio (Mitchison, 1989) and because we recently used this method in an analysis of metaphase and anaphase (Zhai et al., 1995), thus facilitating comparison.

Table II. Rapid Reorganization of Cytoplasmic MTs after NEB

Time Post-NEB*	Cells analyzed	NEB‡	MT reorganization§
min	*No.*	*%*	*%*
0	15	40	0
1	15	100	40
2	15	100	100

*NEB was estimated first by time-lapse phase contrast microscopy of living cells, recording images every 6 s to an OMDR for subsequent playback and analysis. The same cells were then fixed either immediately or 1 or 2 min later and prepared for double immunofluorescence staining.
‡The integrity of the nuclear envelope was assessed by immunostaining for lamin B.
§The status of the cytoplasmic MT network was assessed by immunostaining for tubulin.

Cells were microinjected with a mixture of xrhodamine tubulin and caged-fluorescein tubulin in order to visualize both the total MT array as well as the photoactivated zone. A fluorescent bar was generated using laser irradiation to uncage the fluorescein. Photoactivation of prophase cells under our conditions did not prevent cells from progressing toward mitosis. For the quantitative analysis of fluorescence redistribution, successive images of activated zones were acquired with the CCD at different time intervals after photoactivation.

Cells were analyzed in interphase, prophase pre-NEB, and just post-NEB (Fig. 4). A typical interphase photoactivation experiment using an LLC-PK cell is shown in Fig. 4 *A*. The fluorescent bar can still be seen clearly at 7 min 50 s after activation indicating the relative stability of interphase cytoplasmic microtubules. The kinetics of fluores-

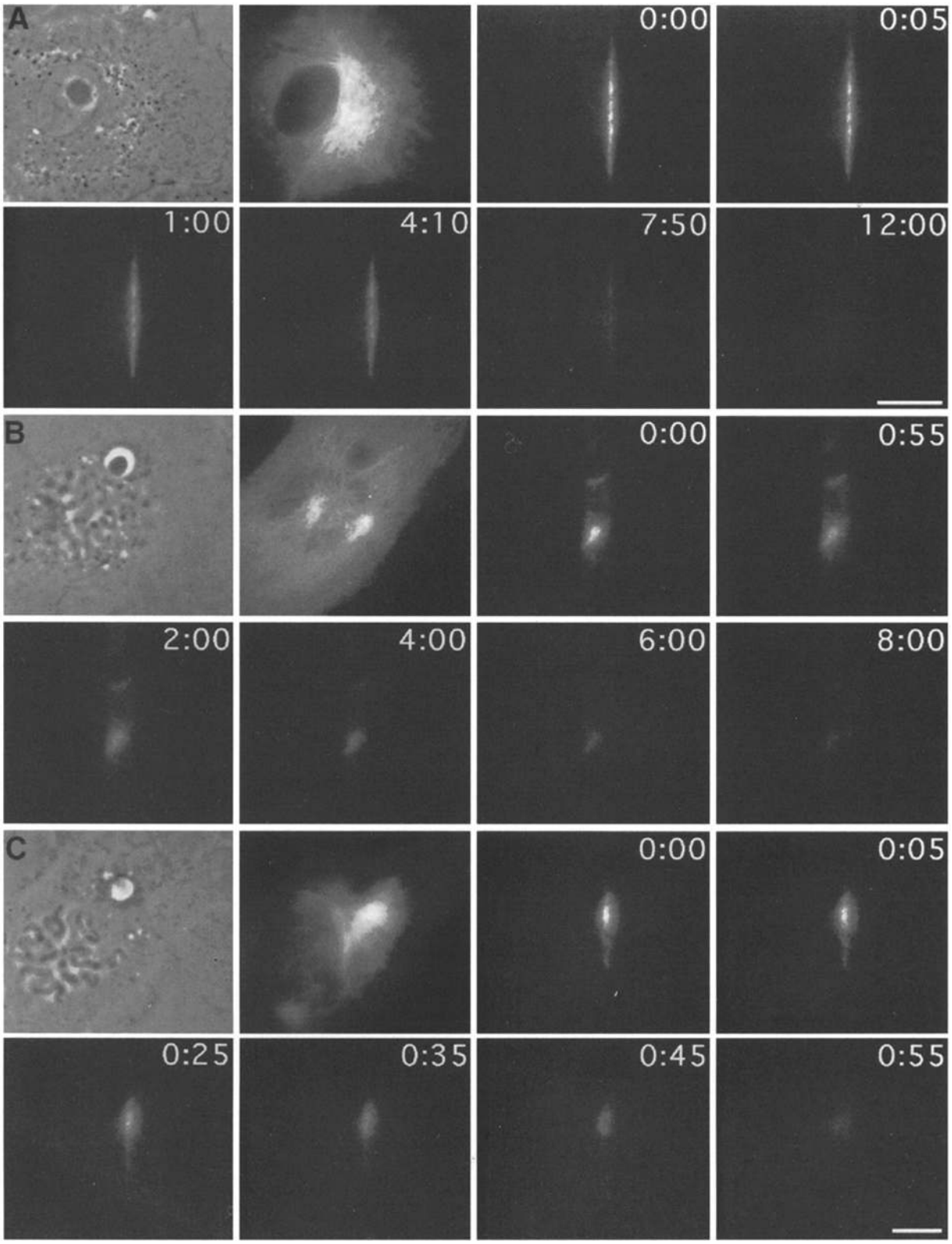

Figure 4. Fluorescence photoactivation imaging to reveal MT dynamics. Cells were injected with a mixture of xrhodamine tubulin and caged-fluorescein tubulin so that the total tubulin as well as the activated zone could be visualized. The phase contrast image is followed by the rhodamine fluorescence image showing the total tubulin in the cell. A fluorescent bar was generated across the MTs using laser irradiation and the first fluorescein image was taken at time 0. The time of each subsequent image is shown in the upper right corner. The interphase cell shown in *A* reveals that it takes several minutes for the MTs in the activated zone to turn over at this stage of the cell cycle. The fluorescent bar can still be detected nearly 8 min after activation. The phase and xrhodamine images in *B* show a cell with the typical prophase morphology before NEB. An area including one of the centrosomes is activated at time 0. Some fluorescence is still detected at the centrosome 8 min later. In *C*, the phase image of this PtK cell shows it to be in late prophase at or just after nuclear envelope breakdown. One of the centrosomal asters is in focus in the rhodamine image and some fluorescence has started to appear within the nucleus indicating that at the time this image was taken, NEB was underway. In less than 1 min after photoactivation, most of the labeled subunits have dissipated from the activated zone, indicating that MT turnover was very rapid. Bar, 10 μm.

Table III. MT Dynamics at Different Stages of the Cell Cycle

	Turnover Half-time (min)				
Cell type	Interphase	Prophase	Post-NEB	Metaphase	
PtK	4.50 ± 1.2*	3.21 ± 0.7	0.73 ± 0.4	nonkMTs	0.68 ± 0.4‡ (17)
	(4)§	(4)	(16)	kMTs	5.30 ± 0.8‡ (17)
LLC-PK	5.75 ± 1.8			nonkMTs	0.90 ± 0.4‡ (15)
	(38)			kMTs	4.70 ± 1.0‡ (15)

*Data taken from Saxton et al. (1984).
‡Data taken from Zhai et al. (1995).
§Number of cells is shown in parentheses.
MT turnover half-times were derived from fluorescence dissipation curves as shown in Fig. 5 and the values obtained from two cell types at different stages of the cell cycle are listed. The cells included in the post-NEB category were activated just after nuclear envelope breakdown like the cell shown in Fig. 4 *C*.

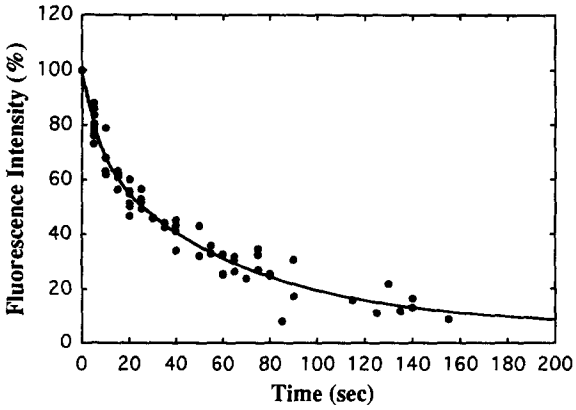

Figure 5. Dissipation of fluorescence after photoactivation post-NEB. Fluorescence photoactivation of MTs in post-NEB cells was carried out as described for Fig. 4 *C*. The fluorescence intensity in a rectangular region enclosing the activated bar was integrated and determined as a function of time after activation. Fluorescence intensities were normalized to 100% at time 0. The data were fit to a double exponential equation, yielding rate constants for two processes, the first interpreted as diffusion of tubulin ($t_{1/2}$ = 5 s) and the second as MT turnover ($t_{1/2}$ = 45 s).

cence dissipation from the activated zone yielded a half-time of MT turnover of 5.75 min (Table III), similar to the value derived from photobleaching studies of interphase PtK cells (Saxton et al., 1984). A prophase pre-NEB cell is shown in Fig. 4 *B*. In this cell, the activated zone included one of the centrosomes as well as some peripheral cytoplasmic MTs. When measured separately, the MTs at the centrosome and those in the cytoplasm were found to turn over at a similar rate. Fluorescence was still detectable 8 min after activation and the kinetics of fluorescence distribution yielded a half-time for MT turnover of 3.2 min (Table III).

In Fig. 4 *C*, a cell from a typical post-NEB photoactivation experiment is shown. The phase image shows the cell in late prophase just before NEB and the xrhodamine fluorescence image (taken the next minute) just before activation, shows the MT pattern characteristic of a cell just post-NEB. Images taken in the fluorescein channel showed that the fluorescence intensity in the activated zone decreased rapidly over a 55-s interval reflecting rapid MT turnover. A phase image taken after this time point confirmed that NEB had occurred. Because of the rapidity of the fluorescence dissipation in the post-NEB cells, a double exponential analysis of the data was undertaken (Fig. 5). Fluorescence intensities showed an initial rapid drop (0–20 s), followed by a slower decrease (20–160 s). The double exponential analysis of the data was consistent with a fast process dissipating with a half-time of 5 s and a slower process with a half-time of 45 s. We interpret the fast process as being the diffusion of fluorescent tubulin subunits away from the activated zone and the slower process as reflecting true MT turnover. This interpretation seems reasonable given the large proportion of monomer present at this stage (see Table I). The time constant for the diffusion process is similar to the 8.8-s half-time that was obtained using photoactivation analysis of tubulin diffusion in melanophore cytoplasm (Rodionov et al., 1994). There was evidence for a small percentage of long-lived fluorescence in some cells. This may have been due to fluorescent vesicles or particles observed in some activated zones, or due to a small population of kinetochore MTs which may be present at this stage. The half-time for MT turnover obtained from curve fitting of the population data (Fig. 5) was nearly identical to the 44-s value obtained from the mean of the individual cells (Table III).

The dissipation of fluorescence from activated zones in PtK metaphase spindles was analyzed in the same manner as described for LLC-PK spindles (Zhai et al., 1995) with the results recorded in Table III. The half-time for nonkMT turnover in PtK spindles (0.68 min) was statistically indistinguishable from the half-time for the centrosomal MTs immediately after NEB (0.73 min).

Discussion

By using a fluorescence ratio assay to measure MT polymer and fluorescence redistribution after photoactivation to measure MT turnover, we find that both levels of MT polymer and dynamic behavior of MTs change significantly during the G_2/M transition, specifically at NEB. While prophase cells had levels of polymer similar to interphase, cells just after NEB had significantly reduced polymer levels which rapidly recovered as MT attachments to kinetochores were made in prometaphase and metaphase. A summary of the changes in MT distribution and polymer levels found during the cell cycle is diagrammed in Fig. 6. Similar changes occurred for MT dynamics. In contrast to interphase, immediately after NEB, MTs exhibited fast turnover. These MTs were initially all centrosomal but became differentiated into kinetochore and nonkinetochore as chromosomes became attached. The dynamics of the nonkinetochore MTs remained rapid but the kinetochore MTs became stabilized. We discuss the pathway for the interphase-mitosis transformation of the MT network. We consider the possibility that the "steady-state" polymer level in mitotic cytoplasm is lower than in interphase, and that in metaphase the polymer level is increased by interaction with the chromosomes, and the implications of these assumptions for spindle morphogenesis.

MT Polymer and Dynamics pre-NEB

During prophase, the number of centrosomal MTs increases and this pattern appears superimposed upon the

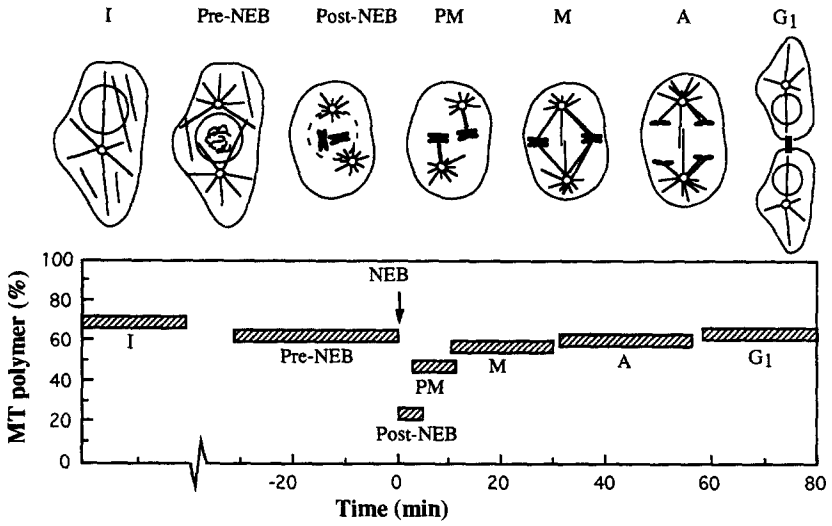

Figure 6. Changes in MT polymer during the cell cycle. (*Upper panel*) Diagram of the changes in morphology of the MT network through the cell cycle. Interphase (I) cell has long MTs, some of which do not converge at the centrosome. The prophase cell (pre-NEB) has an interphase-like network containing two separated centrosomes with increased MT nucleation. The post-NEB cell shows two asters with short MTs. Some astral MTs are captured by kinetochores producing prometaphase (PM) bundles of MTs. With completion of spindle formation at metaphase (M), there is a high density of MTs within the spindle and a reduced number of radiating astral MTs. At anaphase (A), kinetochore MTs depolymerize as chromosomes move toward the pole and astral MTs elongate. Finally, the interphase MT network is reconstituted in G_1. (*Lower panel*) Graph of MT polymer level vs stage of the cell cycle as described above, combining data from Zhai and Borisy (1994) and this study.

cytoplasmic MT network. At some point in prophase, the centrosomes separate and two astral arrays with long microtubules arise. Our data indicate that the level of MT polymer does not change significantly between interphase and prophase even though the number of functional centrosomes doubles. Therefore, this transformation must result from replacement of noncentrosomal MTs by centrosomal ones, resulting most likely from increased nucleation activity of the prophase centrosomes (Kuriyama and Borisy, 1981). Alternatively, release of free MTs from centrosomes (Vorobjev and Chentsov, 1983) may cease in prophase thereby leading to greater retention of MTs at the centrosomes.

Since there are no morphological markers for preprophase cells, there was no way for us to inject preprophase cells in order to measure early prophase MT turnover directly. However, we could compare interphase and prophase cells by measuring MT sensitivity to nocodazole which has been demonstrated to correlate with MT dynamics (Cassimeris et al., 1990; Centonze and Borisy, 1991). Nocodazole apparently binds to tubulin monomers and prevents them from polymerizing onto MTs. If MTs are very dynamic (undergoing frequent cycles of shortening and regrowth), then a brief nocodazole treatment will cause a significant decrease in polymer by preventing the regrowth phase. If MTs are less dynamic and undergo cycles of shortening and regrowth less frequently, then a brief treatment will cause only a small decrease in the polymer level. Our nocodazole experiments indicated that MTs in prophase were only slightly more sensitive to the drug than were interphase cells and the MT pattern that remained was similar to the MT pattern before drug treatment. This result, in combination with the similarity of average MT length, suggests that MT assembly parameters in the cytoplasm are not significantly altered from interphase through prophase until NEB. Data from our photoactivation experiments confirm this view. The MTs of prophase cells with their migrating centrosomes are only slightly more dynamic than MTs in interphase cells and much less dynamic than MTs after NEB. Thus, the difference in organization of the MT network in interphase vs prophase may result primarily from changes in MT nucleation or release from centrosomes. These changes would represent a redistribution of tubulin subunits at essentially constant polymer level. Irrespective of the mechanism, the process of MT reorganization during prophase pre-NEB is gradual. In contrast, the transformation occurring at NEB is singularly abrupt.

While photoactivation and photobleaching analyses are in general agreement when measuring MT turnover in interphase or metaphase cells, discordant results were obtained for prophase cells, with our estimate of MT dynamics pre-NEB being substantially lower than previous determinations. Using photoactivation, we determined that prophase centrosomal MTs turn over with a half-time of 3.2 min, while previous results using photobleaching gave a half-time of only 14 s. We cannot satisfactorily account for this discrepancy, but a major reason may be due to the different ways that the two techniques, photoactivation and photobleaching, report MT dynamics when the amount of polymer at the centrosome is not at steady state. Photoactivation analysis only measures the turnover of MTs existing at the time of photoactivation, while recovery of fluorescence after photobleaching would reflect both the turnover of the existing bleached MTs and any additional fluorescence from new MTs adding to the centrosome because of the increasing MT nucleation capacity of the centrosome that develops during prophase (Kuriyama and Borisy, 1981). Thus, in the case of prophase centrosomes, photobleaching analysis may significantly over estimate the rate of actual MT turnover. If prophase centrosomal MTs actually did turn over as fast as metaphase centrosomal MTs, as the photobleaching studies imply (Saxton et al., 1984), then both classes of MTs would be predicted to be equally sensitive to nocodazole treatment. However, this is not what we observed (see Table I). A brief nocodazole treatment

resulted in the loss of most metaphase astral MTs, but only a minor loss of prophase centrosomal MTs. Therefore, the nocodazole sensitivity experiments confirm the conclusions of the photoactivation analysis that prophase MTs are only slightly more labile than interphase MTs.

MT Polymer and Dynamics at NEB

The sudden loss of the cytoplasmic MT network just following NEB correlated with dramatic changes in both MT polymer and dynamics. Immunofluorescence and direct fluorescence imaging showed a conversion from the long MTs of interphase to many short MTs radiating from the centrosomes. In rare cells, MT fragments were observed scattered throughout the cytoplasm. The scarcity of such cells would imply that MT fragments exist only very transiently post-NEB. Whether these fragments are the result of MT release from the centrosome followed by depolymerization or MT severing activity cannot be determined by immunostaining of fixed cells. In direct fluorescence live imaging observations, MT severing activity was not observed. However, the significance of this negative result is limited because individual MTs were not traceable over extended distances near the center of the cell.

Photoactivation results indicated that the turnover of MTs post-NEB was much faster than in interphase. Nocodazole treatment confirmed that the MTs post-NEB were more labile. However, the most remarkable result was the large drop in polymer. On first consideration, it seems paradoxical that the level of MT polymer decreased just after NEB even though there is increased MT nucleation at the centrosome during prophase. Contrary to the pre-NEB situation, the loss of cytoplasmic MTs is not compensated for by replacement with astral MTs. Moreover, a reduction in length of astral MTs is apparent. Free MTs are not seen and are either no longer produced or are extremely unstable. The decrease in polymer implies a global change to conditions less favorable for MT assembly. The less favorable assembly conditions may persist through metaphase as discussed later.

Studies of cytoplasmic extracts have shown that the presence of active cdc2 kinase results in the loss of long interphase MTs and produces short very dynamic aster MTs (Belmont et al., 1990; Verde et al., 1990, 1992) similar to what we see after NEB. Active cdc2 kinase may transform the MT array by modulating microtubule-associated binding proteins (Ookata et al., 1995) or by activating MT severing proteins (Vale, 1991; McNally and Vale, 1993; Shiina et al., 1992, 1994). Several groups have reported that the cyclin B component of cdc2 kinase is sequestered in the nucleus during prophase (Pines and Hunter, 1991; Gallant and Nigg, 1992), and we have documented that there are dramatic changes in MT distribution and dynamics that occur suddenly after NEB. Together these findings provide circumstantial evidence for a model in which an activity responsible for changes in MT behavior is released from the nucleus at NEB.

Stabilization of MTs by Chromosomes

Remarkably, the abrupt decline of MT polymer at NEB was only a transient one as MT polymer soon returned to pre-NEB levels concomitant with the formation of the bipolar spindle. We interpret this transient drop of MT polymer as resulting from the increase in MT dynamics and an initial lack of kinetochore stabilization of MTs just post-NEB. An accounting of MT dynamics becomes more complicated after NEB as the MTs probe the cytoplasm through cycles of growth and shrinking and encounter the kinetochores of chromosomes. By metaphase, three classes of MTs have developed: astral, nonkinetochore spindle, and kinetochore MTs. Comparison of the kinetics of fluorescence dissipation shows that the turnover half-time of astral MTs in prophase (post-NEB) is similar to that of the nonkinetochore MTs within the metaphase spindle ($t_{1/2} < 1$ min). It is reasonable to think that this level of turnover represents the constitutive level of MT dynamics in mitosis. Capture of MT plus ends by kinetochores correlates with production of a second class of MTs (kinetochore MTs) which are much more stable ($t_{1/2} \sim 5$ min) (Zhai et al., 1995). Thus, our results suggest that the level of MT polymer and MT dynamics in the spindle are tightly coupled to the selective stabilization of MTs by kinetochores as first proposed on the basis of in vitro experiments (Kirschner and Mitchison, 1986).

While we favor the kinetochore as the promoter of MT assembly in the spindle, other experiments have shown that in some meiotic systems chromatin itself can promote MT assembly. When the chromosomes of grasshopper spermatocytes are removed and then rearranged in the spindle with a micromanipulation needle, MT assembly is promoted in the half spindle containing the most chromatin mass regardless of the position or number of kinetochores in the other half spindle (Zhang and Nicklas, 1995). Similarly, chromosomes added to meiotic Xenopus eggs promote MT assembly in their vicinity even in the absence of centrosomes (Karsenti et al., 1984). In contrast, MT assembly promoted by chromosomes has not been observed in the cytoplasm of somatic cells (for review see Rieder et al., 1993). A careful investigation of the polymer levels in monopolar mitotic spindles might sort out the relative role of chromatin and kinetochores in mitosis. If chromatin promotes MT assembly, then the polymer level in monopolar and bipolar spindles should be similar. If bi-oriented kinetochores are the critical factor (see discussion below), then monopolar spindles should contain less polymer then normal bipolar spindles.

Kinetochores and MT Polymer

Can the stabilization of MTs by kinetochores explain the increase in MT polymer seen from NEB to metaphase? The dynamic instability of MTs can be described by four parameters: the velocities of growth and shortening, and the frequencies of transition from growth to shortening and from shortening back to growth. Verde et al. (1992) have presented a mathematical model in which the average length of MTs growing from a nucleating site can be calculated from these four parameters and have shown that the average MT length is very sensitive to the transition frequencies. We have recently (Zhai et al., 1995) presented a release-capture model which accounts for the increased stability of kMTs in terms of a reduction in the probability of MT release from the kinetochore. Assuming that a reduction in the probability of release equates to a

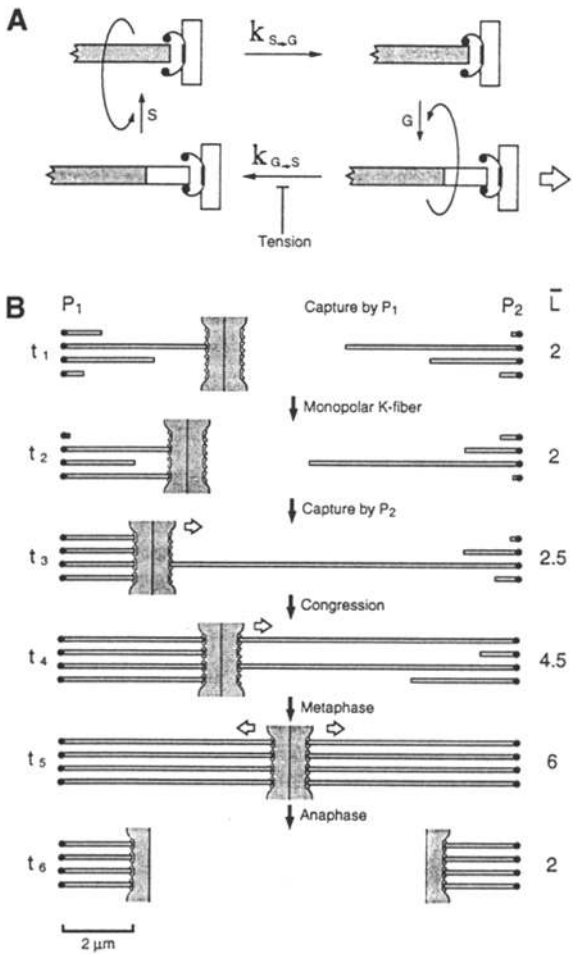

Figure 7. Model of tension-biased microtubule dynamics. (*A*) A single MT with binding proteins of a kinetochore attached to its plus end proceeds through the steps of the dynamic instability cycle: (*S*) shrinking; ($k_{S\text{-}G}$) transition from shrinking to growing; (*G*) growing; and ($k_{G\text{-}S}$) transition from growing to shrinking. Curved arrows indicate that multiple steps of growing or shrinking may occur before a transition to the opposite phase. Tension applied to the kinetochore (*open arrow*) biases dynamics in favor of polymerization by causing the binding proteins to slide along a domain of new MT growth (*open segment*) to the new plus end, and by inhibiting the transition of the MT to the shrinking phase. Should the MT stochastically "attempt" to switch to the shrinking phase, it would be inhibited from detaching from the kinetochore by the stabilizing effect of the MT-binding proteins at its plus end. Thus, new polymer produced by each episode of growth is consolidated and retained while the loss of polymer that would occur at each transition to the shrinking phase is prevented. The resultant effect of tension-biased dynamics is that MTs attached to kinetochores under tension can grow longer than free MTs or kMTs not under tension. If the kinetochore is not under tension or when tension is released, the binding proteins would not be drawn to the new plus end; rather, they would be free to slide down the MT toward the minus end as the MT shortens. (*B*) Schematic diagram showing elevation of MT polymer level in prometaphase by tension applied through bipolar attachments, and loss of MT polymer when tension is released as normally occurs in anaphase. In this diagram, the fate of four centrosomal MTs from each pole are followed as they interact with binding sites on sister kinetochores of a single chromosome. Dynamic centrosomal MTs display a wide distribution of lengths just after NEB (t_1). MT capture from one pole (P_1) causes the chromosome to first move toward P_1 (t_2). The mono-oriented chromosome captures additional MTs until a full complement is attained (t_3) with little or no change in total polymer length (L). A rare long MT from P_2 reaches the chromosome, is captured by the sister kinetochore, and applies tension (*open arrowhead*). Under the influence of this tension, the chromosome begins its congression movement toward the spindle equator (t_4), the tension applied to the trailing kinetochore resulting in an increase in MT polymer by the biased dynamics mechanism outlined in *A*. As additional long MTs from P_2 are captured and held by the sister kinetochore, MT polymer increases further until, at metaphase (t_5), a balance of tension maintains the MTs at an average length of 6 μm, threefold higher than the astral MTs which are still very dynamic with an average length of 2 μm. If tension on the sister kinetochores is released by severing the connection between them (t_6) either experimentally or as normally occurs at anaphase, then each kinetochore moves to a position close to its pole as it did when it was mono-oriented.

reduction in the transition frequency from growth to shortening, this model would predict that the kMTs would be longer than the unprotected, non-kMTs and therefore that MT polymer would become greater in proportion to kinetochore attachment.

We propose that the low MT polymer levels immediately after NEB reflect the steady-state level for isolated centrosomes and tubulin in mitotic cytoplasm. If one could add chromosomes back to the spindle one at a time, we would expect an incremental increase in MT polymer for each chromosome. Actually, the inverse experiment has already been performed; Nicklas and Gordon (1985) extracted chromosomes by micromanipulation from metaphase spermatocyte spindles and found that there was an incremental loss of MT polymer for each chromosome removed. They estimated that only 40% of the original spindle polymer would remain if all chromosomes were removed. In our study we have observed that immediately after NEB (before the attachment of chromosomes), the polymer level was less than half that found at metaphase, consistent with the EM determinations of Nicklas and Gordon (1985).

However, this apparent excellent agreement is not the total story. The study of Nicklas and Gordon (1985) removed chromosomes from bipolar spindles; that is, the kinetochores were attached to both poles. A different conclusion comes from analysis of monopolar spindles. In monopolar spindles, the kinetochores are located near the centrosome and their kMTs are not longer than the non-kMTs, even though photobleaching evidence shows that they are as stable as the kMTs in bipolar spindles (Cassimeris et al., 1994). Thus, monopolar spindles show clearly that capture and stabilization of MTs by the kinetochore do not automatically equate to greater lengths of these MTs. The comparison of results with monopolar and bipolar spindles suggests an additional factor is involved in determining MT length and polymer level.

An additional factor in spindle morphogenesis is tension. How might tension at the kinetochore determine MT length and polymer levels? A recent model (Lombillo et al., 1995; Desai and Mitchison, 1995) for the mechanism of kinetochore motility involves a depolymerization-driven process and proposes that kinetochore coupling proteins bound to the outer surface of the plus end of MTs prevent

depolymerization past the point of attachment. However, thermal energy may cause the coupling proteins and the kinetochore to slide down the MT lattice and allow depolymerization to occur down to this new location. As this cycle is repeated, the kinetochore moves toward the minus end of the MT as it depolymerizes without losing its attachment to the MT end. We propose that under steady-state conditions there can be tension-driven polymerization by a similar mechanism (Fig. 7). In this model, the same coupling proteins are bound to the outer surface of the plus end of the MT. When the MT undergoes a period of growth, tension on the kinetochore causes it to slide along the MT lattice so that it keeps moving with the growing plus end. When the MT undergoes an incipient transition to the shortening phase, it is immediately rescued by the attached coupling proteins, since the MT cannot depolymerize past this point. Tension on the kinetochore maintains the MT at its new length until it again makes a transition to the growing phase and resumes elongation. The kinetochore will again move to the new plus end position consolidating the incremental growth. In this way, the tension may regulate the assembly and disassembly of kMTs at their kinetochore attachment sites (Skibbens et al., 1993). Therefore, kinetochores under tension can increase the amount of MT polymer over what would be found if the kinetochore were free to slide down the MT lattice toward the minus end as the MT depolymerized. The obverse of the proposed MT-promoting activity of tension has been observed when tension on sister kinetochores of a bi-oriented chromosome was released by severing the connection between them with a laser (Skibbens et al., 1995). Both sister kinetochores then moved toward their respective poles accompanied by the shortening of both kinetochore fibers, with the resulting reduction of the MT polymer originally present in those kinetochore fibers. We propose that bi-oriented chromosome attachment not only stabilizes MTs, but actually promotes assembly to an elevated "meta-stable" level through tension that is exerted on the kinetochore MTs. When chromatids split at anaphase, this tension is released and kinetochore MTs depolymerize. Thus, the shift to depolymerization conditions that we previously looked for at anaphase onset (Zhai and Borisy, 1994) may actually occur at NEB.

We thank John Peloquin for preparation of derivatized tubulin and valuable discussions throughout this study. We would like also to thank Dr. Tim J. Mitchison for his gift of caged-fluorescein probe.

This work was supported by National Institutes of Health grant GM 25062 to G.G. Borisy.

Received for publication 18 August 1995 and in revised form 19 June 1996.

References

Aubin, J.E., M. Osborn, and K. Weber. 1980. Variations in the distribution and migration of centriole duplexes in mitotic PtK_2 cells studied by immunofluorescence microscopy. *J. Cell Sci.* 43:177–194.

Belmont, L.D., A.A. Hyman, K.E. Sawin, and T.J. Mitchison. 1990. Real-time visualization of cell cycle-dependent changes in microtubule dynamics in cytoplasmic extracts. *Cell.* 62:579–589.

Cassimeris, L., C.L. Rieder, G. Rupp, and E.D. Salmon. 1990. Stability of microtubule attachment to metaphase kinetochores in PtK_1 cells. *J. Cell Sci.* 96: 9–15.

Cassimeris, L., C.L. Rieder, and E.D. Salmon. 1994. Microtubule assembly and kinetochore directional instability in vertebrate monopolar spindles: implications for the mechanism of chromosome congression. *J. Cell Sci.* 107:285–297.

Centonze, V.E., and G.G. Borisy. 1991. Pole-to-chromosome movements induced at metaphase: sites of microtubule disassembly. *J. Cell Sci.* 100:205–211.

Coue, M., V.A. Lombillo, and J.R. McIntosh. 1991. Microtubule depolymerization promotes particle and chromosome movement in vitro. *J. Cell Biol.* 112: 1165–1175.

DeBrabander, M., G. Geuens, J. DeMay, and M. Joniau. 1979. Light microscopic and ultrastructural distribution of immunoreactive tubulin in mitotic mammalian cells. *Biol. Cell.* 34:213–226.

Desai, A., and T.J. Mitchison. 1995. A new role for motor proteins as couplers to depolymerizing microtubules. *J. Cell Biol.* 128:1–4.

Gallant, P., and E. A. Nigg. 1992. Cyclin B2 undergoes cell cycle dependent nuclear translocation and, when expressed as a non-destructible mutant, causes mitotic arrest in Hela cells. *J. Cell Biol.* 117:213–224.

Gelfand, V.I., and A.D. Bershadsky. 1991. Microtubule dynamics: mechanism, regulation, and function. *Annu. Rev. Cell Biol.* 7:93–116.

Gorbsky, G.J., P.J.Sammak, and G.G. Borisy. 1987. Chromosomes move poleward in anaphase along stationary microtubules that coordinately disassemble from their kinetochore ends. *J. Cell Biol.* 104:9–18.

Inoué, S., and H. Sato. 1967. Cell motility by labile association of molecules: the nature of mitotic spindle fibers and their role in chromosome movement. *J. Gen. Physiol.* 50:259–292.

Karsenti, E., S. Kobayashi, T. Mitchison, and M. Kirschner. 1984. Role of the centrosome in organizing the interphase microtubule array: properties of cytoplasts containing or lacking centrosomes. *J. Cell Biol.* 98:1763–1776.

Koshland, E.D., T.J. Mitchison, and M.W. Kirschner. 1988. Polewards chromosome movement driven by microtubule depolymerization in vitro. *Nature (Lond.).* 33:499–504.

Kirschner, M., and T. Mitchison. 1986. Beyond self-assembly: from microtubules to morphogenesis. *Cell.* 45:329–342.

Kuriyama, R., and G.G. Borisy. 1981. Microtubule nucleating activity of centrosomes in Chinese hamster ovary cells is independent of the centriole cycle but coupled to the mitotic cycle. *J. Cell Biol.* 91:822–826.

Lombillo, V.A., C. Nislow, T.J. Yen, V.I. Gelfand, and J.R. McIntosh. 1995. Antibodies to the kinesin motor domain and CENP-E inhibit microtubule depolymerization-dependent motion of chromosomes in vitro *J. Cell Biol.* 128:107–115.

Margolis, R.L., and L. Wilson. 1981. Microtubule treadmills: possible molecular machinery. *Nature (Lond.).* 293:705–711.

McNally, F.J., and Vale R.D. 1993. Identification of katanin, an ATPase that severs and disassembles stable microtubules. *Cell.* 75:419–429.

Merdes, A., E.H.K. Stelzer, and J. De May. 1991. The three-dimensional architecture of the mitotic spindle, analyzed by confocal fluorescence and electron microscopy. *J. Elec. Micr. Tech.* 18:61–73.

Mitchison, T.J. 1989. Polewards microtubule flux in the mitotic spindle: evidence from photoactivation of fluorescence. *J. Cell Biol.* 109:637–652.

Nicklas, R.B., and G.W. Gordon. 1985. The total length of spindle microtubules depends on the number of chromosomes present. *J. Cell Biol.* 100:1–7.

Ookata, K., S. Hisanaga, J.C. Bulinski, H. Murofushi, H. Aizawa, T.J. Itoh, H. Hotani, E. Okumura, K. Tachibana, and T. Kishimoto. 1995. Cyclin B interaction with microtubule-associated protein 4 (MAP4) targets $p34^{cdc2}$ kinase to microtubules and is a potential regulator of M-phase microtubule dynamics. *J. Cell Biol.* 128:849–862.

Pepperkok, R., M.H. Bré, J. Davoust, and T.E. Kreis. 1990. Microtubules are stabilized in confluent epithelial cells but not in fibroblasts. *J. Cell Biol.* 111: 3003–3012.

Pines, J., and T. Hunter. 1991. Human cyclins A and B1 are differentially located in the cell and undergo cell cycle–dependant nuclear transport. *J. Cell Biol.* 115:1–17.

Rattner, J.B., and M.W. Berns. 1976. Distribution of microtubules during centriole separation in rat kangaroo cells. *Cytobios.* 15:37–43.

Rieder, C.L., J.G. Ault, U. Eichenlaub-Ritter, and G. Sludder. 1993. Morphogenesis of the mitotic and meiotic spindle: conclusions obtained from one system are not necessarily applicable to the other. *In* Chromosome Segregation and Aneuploidy. B.K. Vig, editor. NATO ASI Series. Vol. H72. Springer-Verlag, Berlin Heidelberg, FRG. pp. 183–197.

Rodionov, V.I., S.S. Lim, V.I. Gelfand, and G.G. Borisy. 1994. Microtubule dynamics in fish melanophores. *J. Cell Biol.* 126:1455–1464.

Sammak, P.J., G. J. Gorbsky, and G.G. Borisy. 1987. Microtubule dynamics in vivo: a test of mechanisms of turnover. *J. Cell Biol.* 104:395–405.

Saxton, W.M., D.L. Stemple, R.J. Leslie, E.D. Salmon, M. Zavortink, and J.R. McIntosh. 1984. Tubulin, dynamics in cultured mammalian cells. *J. Cell Biol.* 99:2175–2186.

Shiina, N., Y. Gotoh, and E. Nishida. 1992. A novel homo-oligomeric protein responsible for an MPF-dependent microtubule severing activity. *EMBO (Eur. Mol. Biol. Organ.) J.* 11:4723–4731.

Shiina, N., Y. Gotoh, N. Kubomura, A. Iwamatsu, and E. Nishida. 1994. Microtubule severing by elongation factor 1α. *Science (Wash. DC)* 266:282–285.

Skibbens, R.V., V.P. Skeen, and E.D. Salmon. 1993. Directional instability of kinetochore motility during chromosome congression and segregation in mitotic Newt Lung cells: a push-pull mechanism. *J. Cell Biol.* 859–875.

Skibbens, R.V., C.L. Rieder, and E.D. Salmon. 1995. Kinetochore motility after severing between sister centromeres using laser microsurgery: evidence that kinetochore directional instability and position is regulated by tension. *J. Cell Sci.* 108(7):2537–2548.

Vale, R.D. 1991. Severing of stable microtubules by a mitotically activated protein in Xenopus egg extracts. *Cell.* 64:827–839.

Vandre, D.D, and G.G. Borisy. 1986. The interphase-mitosis transformation of the microtubule network in mammalian cells. *In* Cell Motility: Mechanism and Regulation. H. Ishikawa, S. Hatano, and H. Sato, editors. Alan R. Liss, Inc., NY. pp. 389–401.

Vandre, D.D., P. Kronebusch, and G.G. Borisy. 1984. The interphase-mitosis transition: microtubule rearrangements in cultured cells and sea urchin eggs. *In* The Molecular Biology of the Cytoskeleton. G.G. Borisy, D.W. Cleveland, and D. Murphy, editors. Cold Spring Harbor Laboratory Press, Cold Spring Harbor, NY. pp. 3–16.

Verde, F., J. Labbé, M. Dorée, and E. Karsenti. 1990. Regulation of microtubule dynamics by cdc2 protein kinase in cell-free extracts of Xenopus eggs. *Nature (Lond.).* 343:233–238.

Verde, F., M. Dogterom, E. Stelzer, E. Karsenti, and S. Leibler. 1992. Control of microtubule dynamics and length by cyclin A- and cyclin B- dependent kinases in Xenopus egg extracts. *J. Cell Biol.* 118:1097–1108.

Vorobjev, I.A., and Y.S. Chentsov. 1983. The dynamics of reconstitution of microtubules around the cell center after cooling. *Eur. J. Cell Biol.* 30:149–153.

Waters, J.C., R.W. Cole, and C.L. Rieder. 1993. The force-producing mechanism for centrosome separation during spindle formation in vertebrates is intrinsic to each aster. *J. Cell Biol.* 122:361–372.

Zhai, Y., and G.G. Borisy. 1994. Quantitative determination of the proportion of microtubule polymer during the mitosis-interphase transition. *J. Cell Sci.* 107(4):881–890.

Zhai, Y., P.J. Kronebusch, and G.G. Borisy. 1995. Kinetochore microtubules dynamics and the metaphase-anaphase transition. *J. Cell Biol.* 131:721–734.

Zhang, D., and R.B. Nicklas. 1995. The impact of Chromosomes and centrosomes on spindle assembly as observed in living cells. *J. Cell Biol.* 129: 1287–1300.